

pubs.acs.org/JPCB Article

# Spectroscopic and Structural Characterization of Water-Shared Ion-Pairs in Aqueous Sodium and Lithium Hydroxide

Published as part of The Journal of Physical Chemistry virtual special issue "Lawrence R. Pratt Festschrift". Denilson Mendes de Oliveira, Aria J. Bredt, Tierney C. Miller, Steven A. Corcelli, and Dor Ben-Amotz\*



Cite This: J. Phys. Chem. B 2021, 125, 1439-1446



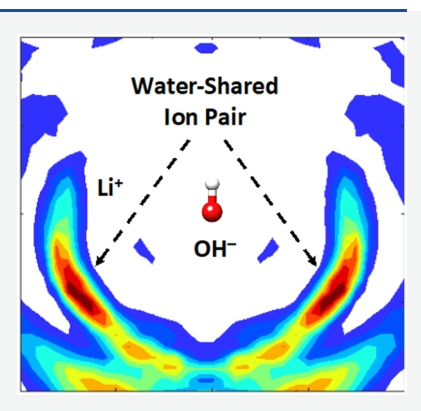
**ACCESS** 

III Metrics & More



Supporting Information

ABSTRACT: The structures of the ion-pairs formed in aqueous NaOH and LiOH solutions are elucidated by combining Raman multivariate curve resolution (Raman-MCR) experiments and *ab initio* molecular dynamics (AIMD) simulations. The results extend prior findings to reveal that the initially formed ion-pairs are predominantly water-shared, with the hydroxide ion retaining its full first hydration-shell, while direct contact ion-pairing only becomes significant at higher concentrations. Our results confirm previous experiments and simulations indicating greater ion-pairing in aqueous LiOH than NaOH as well as at high temperatures. Our results further imply that NaOH and LiOH ion-pairing free energies have an approximately linear (rather than square-root) dependence on ion concentration (in the molar range), with positive enthalpies and entropies that increase with concentration, thus implying that water-mediated interactions enthalpically disfavor and entropically favor ion-pair formation.



### **■ INTRODUCTION**

The tactile slipperiness and chemical activity of alkaline water are linked to the influence of hydroxide (OH<sup>-</sup>) ions and their countercations on water structure and dynamics. 1-8 The influence of the countercation is evidenced, for example, by the marked differences between the conductivity<sup>2,3</sup> and proton transfer dynamics in aqueous NaOH and LiOH. Although these differences are due in part to the greater abundance of ion-pairs in LiOH solutions, as well as in both solutions at higher temperatures, 2,3,5,8 open questions remain as to whether the corresponding ion-pairs are best characterized as direct, water-shared, or water-separated, depending on whether there are 0, 1, or 2 water molecules, respectively, between the paired counterions.9 To address this question, as well as to spectroscopically, structurally, and thermodynamically quantify ion-pairing in aqueous NaOH and LiOH solutions, we have performed Raman multivariate curve resolution (Raman-MCR)<sup>10</sup> experiments and ab initio molecular dynamics (AIMD) simulations. Our results confirm that strong HOH···OH hydrogen bonds stabilize the first hydrationshell of OH<sup>-</sup> and thus favor the formation of water-shared ionpairs between Na<sup>+</sup> or Li<sup>+</sup> and hydrated OH<sup>-</sup>. Moreover, our concentration and temperature dependent measurements imply that the ion-pairing free energies have an approximately linear (rather than square-root) concentration dependence and are enthalpically disfavored and entropically favored to a degree that increases with increasing concentration.

The present results may be viewed as extending a recently reported Raman-MCR and AIMD study, as well as prior ion-

 $pairing^{8,11-16}$  and hydration  $^{17-21}$  studies, to better characterize and quantify ion-pairing in aqueous NaOH and LiOH solutions. Our conclusion that the tightly bound hydrationshell of OH- promotes water-shared ion-pairing is complementary to a recent Raman study of aqueous MgCl2 and LaCl3 that attributed water-shared ion-pairing to the tightly bound hydration-shells of the multivalent cations. 16 More generally, the high solubility of ions in water implies that ion-water interactions can overcome the intrinsic attraction of counterions for each other. Such water-mediated interaction may in some cases even facilitate the pairing of like-charged ions in water and at air—water interfaces. <sup>22–24</sup> Our results add to the associated intrigue by revealing that ion-pairing can be entropically rather than enthalpically favored, thus providing further evidence that water-mediated interactions may be more significant facilitators of ion-pairing than the electrostatic interactions between ions.

# EXPERIMENTAL MEASUREMENT AND ANALYSIS METHODS

Aqueous solutions of NaOH (sodium hydroxide, ACROS Organics, 98.5%) and LiOH (lithium hydroxide, Sigma-

Received: November 24, 2020 Revised: January 21, 2021 Published: January 29, 2021





Aldrich, 98%) were prepared with ultrapure filtered water (Milli-Q UF Plus, Millipore, 18.2 M $\Omega$  cm). Raman spectra were obtained using an Ar-ion 514.5 nm laser with ~20 mW of power at the sample and 5 min of integration time, as previously described.<sup>25</sup> Briefly, backscattered Raman photons were collected from the sample using a 20× long-workingdistance microscope objective (NA = 0.42, Mitutoyo Inc.) and transmitted with an optical fiber bundle to an imaging spectrograph (SpectraPro300i, Acton Research Inc.) equipped with a 300 grooves/mm grating and a thermoelectrically cooled CCD camera (Princeton Instruments Inc.).

Raman spectra were obtained at concentrations between 0.25 and 2 M at temperatures of 5, 10, and 20  $^{\circ}$ C, for LiOH, as well as at 40 °C for NaOH. For NaOH at 5 °C, spectra were obtained over a wider concentration range of 0.25-10 M. In addition, temperature dependent spectra were obtained from 0.5 M LiOH and NaOH solutions over a 0-100 °C temperature range. The measured spectra were all smoothed using a 15 point Savitzky-Golay filter. The spectra were subsequently treated using self-modeling curve resolution (SMCR) decomposition 10,26-28 to obtain minimum-area non-negative solute-correlated (SC) spectra from pairs of pure water and solution spectra collected under identical experimental conditions at ambient pressure and temperatures regulated to within <0.1 °C. The minimum-area constraint was applied in the spectral region between 2000 and 4000 cm<sup>-1</sup> after subtraction of a broad low-intensity background using a fourth order polynomial fit to baseline points adjacent to the OH stretch band (see SI Figure S3). The SC spectra were divided by the corresponding total hydroxide concentration, so that the resulting SC spectra are effectively normalized to the same concentration.

Estimates of the ion-pairing association constants in aqueous NaOH and LiOH were obtained from the SC intensities near 3500 cm<sup>-1</sup> (determined as described in the SI) which are found to decrease strongly upon ion-pair formation. Thus, the fraction of free (non-ion-paired) hydroxide ions,  $x_{\rm F}$ , may be experimentally estimated using eq 1, which equates  $x_F$  with the ratio of the measured intensity I of the normalized SC spectrum at a given concentration  $c_T = [MOH]_T$  (where M = Na or Li) and the intensity  $I_0$  in the dilute limit, at which the ions are assumed to be completely dissociated.

$$x_{\rm F} = \frac{{\rm [OH^-]_F}}{c_{\rm T}} = \frac{{\rm [M^+]_F}}{c_{\rm T}} \approx \frac{I}{I_0}$$
 (1)

The dissociated fraction  $x_{\rm F}$ , pertaining to an ion-pairing equilibrium of the form  $M^+ + OH^- \rightleftharpoons MOH$ , may further be related to the ion-pairing association constant  $K_A$  as follows.

$$x_{\rm F} = \frac{-1 + \sqrt{1 + 4K_{\rm A}c_{\rm T}}}{2K_{\rm A}c_{\rm T}} \tag{2}$$

Note that we define the equilibrium constant as a ratio of concentrations (not activities). Thus, at higher concentrations,  $K_A$  is expected to be concentration dependent. As we will see, our experimental results imply that the corresponding free energy  $\Delta G = -RT \ln(K_A)$  has an approximately linear concentration dependence, thus implying that  $K_A$  is described by eq 3, in which  $K_0$  is the association constant at infinite dilution and the coefficient b dictates the linear concentration dependence of  $\Delta G = \Delta G_0 - RT(bc_T)$ , with  $\Delta G_0$  corresponding to the ion-pairing free energy (potential of mean force) at infinite dilution.

$$K_{\rm A} = K_0 \exp(bc_{\rm T}) \tag{3}$$

Equations 2 and 3 may thus be used to obtain  $K_0$  and b by fitting the experimentally determined  $x_{\rm F}$  as a function of  $c_{\rm T}$  (as described in greater detail in the SI).

The ion-pairing thermodynamic functions are related to  $K_A$ and its temperature dependence, as follows.

$$\Delta G = -RT \ln(K_{\rm A}) \tag{4}$$

$$\Delta S = -\left(\frac{\partial \Delta G}{\partial T}\right)_{\rm p} \tag{5}$$

$$\Delta H = \Delta G + T \Delta S \tag{6}$$

#### ■ SIMULATION METHODS

Simulation boxes of 1 M LiOH and 1 M NaOH were built with Packmol, <sup>29</sup> where each system contains 110 H<sub>2</sub>O, 2 OH<sup>-</sup>, and 2 countercations. Ab initio molecular dynamics (AIMD) simulations were performed utilizing the CP2K open source molecular dynamics package.<sup>30</sup> To start, a short geometry optimization of the atomic coordinates was performed before DFT-based AIMD equilibration (20 ps) and production (200 ps) in the NVT ensemble, similar to the protocol previously used for studying excess protons in water. 31,32 Born-Oppenheimer molecular dynamics were implemented to propagate the nuclei with a time step of 0.5 fs. CP2K uses the Quickstep method for force evaluations wherein the Gaussian and plane waves scheme is utilized.<sup>33</sup> We implemented the Goedecker-Teter-Hutter (GTH) pseudopotentials<sup>34–36</sup> for treatment of the core electrons, the TZVP-GTH basis set, and the BLYP functional<sup>37,38</sup> for exchangecorrelation contributions with Grimme's D3 correction.<sup>35</sup>

Cylindrical Distribution Functions. The often-used radial distribution function loses or hides a large amount of structural information about the solvation environment when applied to molecules with a nonspherical symmetry. By introducing a second dimension to the distribution function, such as one along a bond axis, a two-dimensional mapping of the solvation environment around a cylindrical molecule can be calculated, i.e., a cylindrical distribution function (CDF).<sup>40</sup> The CDF, g(r, z), depends on the radius of a ring, r, around the molecule of interest, and a "height" of the particle of interest in a plane about the central atom, z. Here, the CDFs are centered on the hydroxide ion; thus, the "height" parameter is defined as

$$z = \hat{\nu}_{\text{OH}} \cdot \vec{\nu}_{\text{O}i} \tag{7}$$

where  $\hat{v}_{OH}$  is the unit vector from the hydroxide oxygen (defined as the r = 0, z = 0 position) to the hydroxide hydrogen, and  $\vec{v}_{Oi}$  is a vector from the central oxygen atom to the particle of interest. The radius of the ring for the particle of interest can then be obtained by

$$\vec{r} = \vec{\nu}_{\text{Oi}} - z\hat{\nu}_{\text{OH}} \tag{8}$$

which gives the inner radius of a ring around the hydroxide oxygen that is shifted up or down by z. Each unique combination of r and z defines a ring around OH in which counterions or solvent molecules can reside. The resultant data set is visualized as a two-dimensional histogram in which the value at each (r, z) location represents the total population in the ring of radius r and displaced along the O-H axis by a distance z with respect to the oxygen atom.

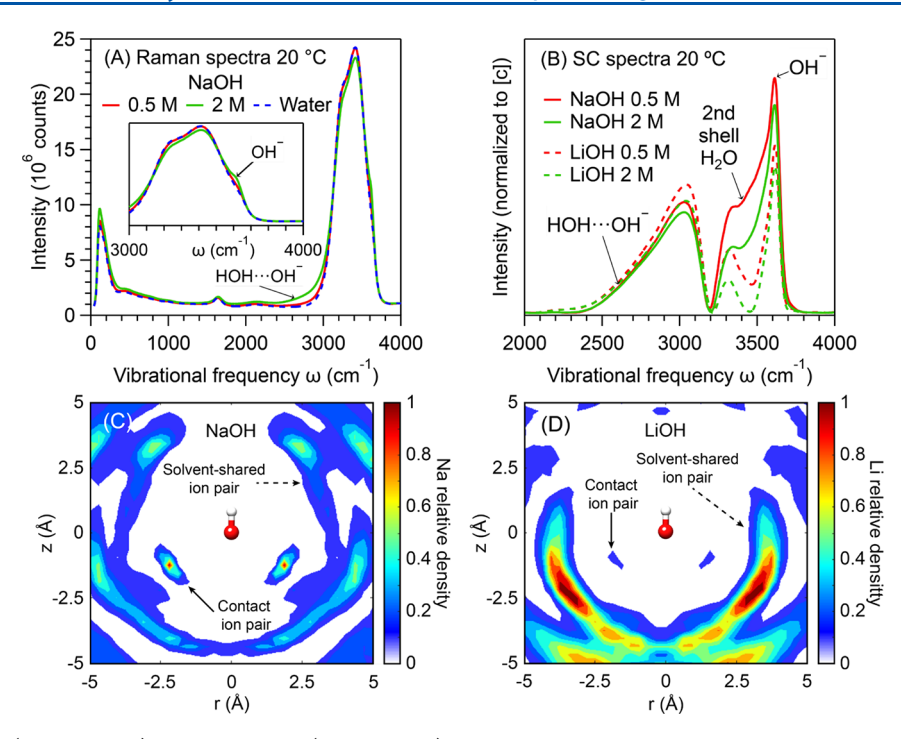


Figure 1. Experimental (upper panels) and simulation (lower panels) results for aqueous NaOH and LiOH. Experimental Raman spectra of aqueous NaOH (A) and Raman-MCR of aqueous NaOH and LiOH (B) at 20  $^{\circ}$ C and both 0.5 and 2 M. AIMD predictions of the distributions of Na $^{+}$  (C) and Li $^{+}$  (D) around OH $^{-}$  at 1 M and 25  $^{\circ}$ C. See the experimental and simulation methods for further details.

#### RESULTS

Figure 1 contains experimental (upper panels) and simulation (lower panels) results pertaining to aqueous NaOH and LiOH solutions. Figure 1A compares Raman spectra of pure water and aqueous NaOH, all of which look quite similar, although the 2 M NaOH solution spectra show evidence of an emerging OH<sup>-</sup> stretch peak near 3600 cm<sup>-1</sup> and a low-frequency OH tail below 3000 cm<sup>-1</sup>. These features are more clearly evident in the SC spectra shown in panel B obtained from 0.5 and 2 M solutions at 20 °C, normalized to the same concentration (as described above). The normalization procedure highlights concentration dependent changes resulting from ion-pairing, as all the normalized SC spectra would look identical if the ions remained fully dissociated. Note that such SC spectra may in general contain vibrational features arising from water molecules whose vibrations are perturbed by one or both of the counterions of NaOH and LiOH, as well as the OH stretch vibration of OH- itself, which gives rise to the relatively sharp peak near 3600 cm<sup>-1</sup>.<sup>1,41</sup> The remaining hydration-shell features that appear in the SC spectra in Figure 1B are assigned with the aid of AIMD simulations.

The broad low-frequency feature in the SC spectra in Figure 1B is assigned to HOH···OH<sup>-</sup> water molecules directly hydrogen bonded to OH<sup>-</sup>. The nearly constant intensity of this low-frequency tail in all these normalized SC spectra indicates that the first hydration-shell of OH<sup>-</sup> is strongly bound, thus suppressing the formation of direct contact ion-pairs between OH<sup>-</sup> and either Na<sup>+</sup> or Li<sup>+</sup> over this concentration range. The latter conclusion is consistent with the predicted distributions of Na<sup>+</sup> and Li<sup>+</sup> around OH<sup>-</sup> at 1 M, shown in Figure 1C,D, which indicate that water-shared ion-pairs far outnumber direct contact ion-pairs. Further support for this conclusion is provided by our additional AIMD simulation predictions that OH<sup>-</sup> remains essentially fully

hydrated in both 1 M NaOH and LiOH aqueous solutions (see SI Figures S4 and S5).

The simulation results shown in Figure 1D further reveal that the cations in the water-shared ion-pairs are located about 3 Å away from OH<sup>-</sup>, consistent with the ion-pairing-induced displacement of water molecules from the second hydration-shell of OH<sup>-</sup>. Note that water-separated (rather than water-shared) ion-pairs, in which both the cation and anion retain their first hydration-shell, would have a larger cation—anion separation of at least 5 Å. Moreover, the structure and spectra of the hydration-shell water molecules around such water-separated ion-pairs would be expected to resemble the corresponding fully hydrated ions, and thus, Raman-MCR is expected to be relatively insensitive to water-separated ion-pairing.

Water-shared ion-pairing, on the other hand, should significantly alter the ion-pair hydration-shell structure and spectra. The concentration dependent decrease in the hydration-shell intensity near 3500 cm<sup>-1</sup>, shown in Figure 1B, is thus assigned to the ion-pairing-induced displacement of second hydration-shell water molecules around OH<sup>-</sup>. This assignment is supported by the fact that the vibrational frequencies of such second hydration-shell water molecules are predicted to occur in this spectral region. Moreover, the OH population whose frequency is near 3500 cm<sup>-1</sup> is similar to that of water molecules directly hydrogen bonded to large anions such as I<sup>-</sup>. Thus, the hydrogen bonds donated from the second hydration-shell water molecules to the hydrated OH<sup>-</sup> are apparently similar in strength to those of water molecules directly hydrogen bonded to I<sup>-</sup>.

The SC spectral comparisons in Figure 1B further imply that there are fewer water-shared ion-pairs in NaOH than in LiOH, as indicated by the larger intensity near 3500 cm<sup>-1</sup> in NaOH than in LiOH. The greater ion-pairing propensity of LiOH than NaOH is also consistent with the simulation results

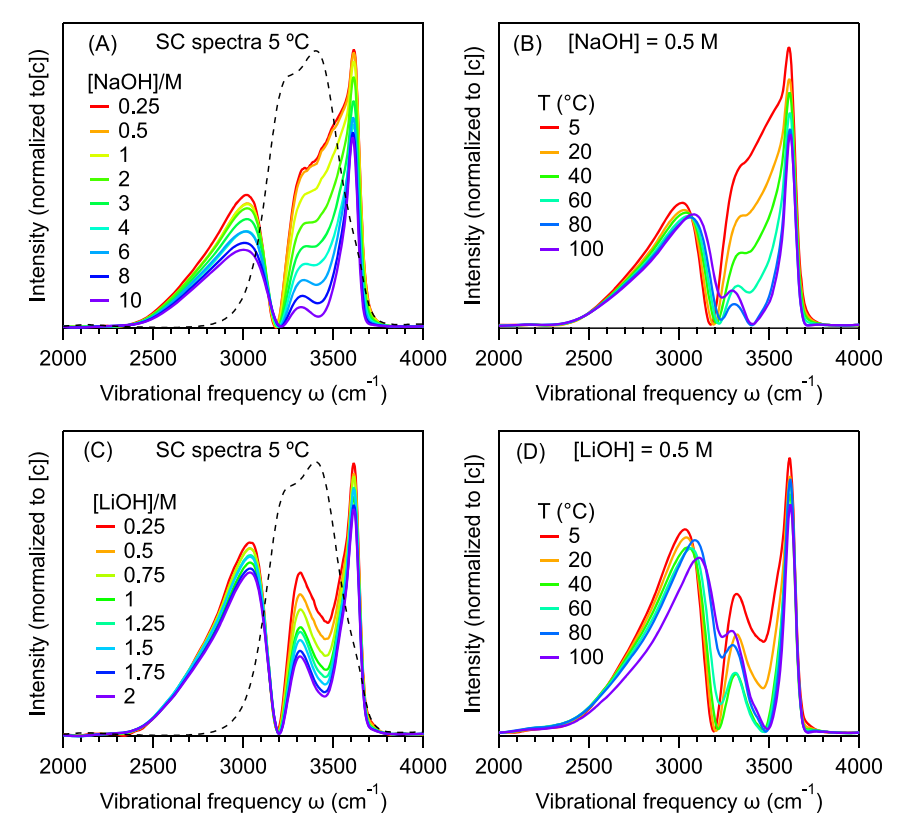


Figure 2. Comparison of the concentration (A, C) and temperature (B, D) dependent Raman-MCR hydration-shell spectra of aqueous NaOH (A, B) and LiOH (C, D). The dashed curves are pure water spectra at the specified temperatures (scaled to approximately the same peak intensity).

shown in Figure 1C,D, as well as with prior potentiometric measurements indicating that the ion-pairing association constant of LiOH is about 3 times larger than that of NaOH.<sup>2</sup>

Although Na<sup>+</sup> has little influence on the vibrational spectrum of water, 42 that is not the case for the higher-charge-density Li+ cation, whose hydration-shell spectrum gives rise to an SC OH stretch band extending from ~3000 to 3500 cm<sup>-1</sup> (see SI Figure S10 for ref 31). Thus, while the SC spectrum of NaOH is due primarily to OH and its hydration-shell, the LiOH SC spectrum is also influenced by the hydration-shell of Li<sup>+</sup>. Nevertheless, any concentration dependent changes in the SC spectra of either NaOH or LiOH must necessarily result from the formation of ion-pairs (since the infinitely dilute SC spectra pertain to two separated and fully hydrated ions). It has previously been suggested that the observed Raman intensity decrease in aqueous NaOH and LiOH near 3500 cm<sup>-1</sup> may be influenced by a decrease in the Raman cross-section of the ionpair hydration-shell waters. Although such a cross-section decrease is plausible, the observed intensity decrease is also consistent with that expected to result from the displacement of OH- second hydration-shell waters by the cation and its remaining first hydration-shell waters.

Figure 2 compares the concentration and temperature dependence of the SC spectra of aqueous NaOH and LiOH. The qualitative similarity of the NaOH SC spectra in Figure 2A,B, particularly over the 3200–3500 cm<sup>-1</sup> spectral range, implies that the increase in NaOH ion-pairing between 0.25 and 10 M (at 5 °C) is similar to that in a 0.5 M solution over a temperature range of 5 and 100 °C. The nearly zero intensity near 3500 cm<sup>-1</sup> in the highest concentration and temperature SC spectra implies that an aqueous NaOH solution is

essentially completely ion-paired both at 10 M and 5  $^{\circ}\text{C}$  and at 0.5 M and 100  $^{\circ}\text{C}.$ 

The concentration dependence of the lower-frequency HOH···OH<sup>-</sup> tail shown in Figure 2A differs somewhat from that of the temperature dependent spectra in Figure 2B. Specifically, Figure 2A reveals a concentration dependent decrease in the area of the broad low-frequency OH band, indicating that at concentrations above 2 M some of the water molecules directly bound to OH- are displaced by Na+, implying the formation of some direct contact ion-pairs at such high concentrations, as previously determined using X-ray diffraction measurements. On the other hand, the temperature dependent spectra in Figure 2B reveal that the low-frequency OH tail has an area that is nearly temperature independent, thus indicating that there are few direct contact ion-pairs in 0.5 M NaOH even at 100 °C, where the solution consists almost entirely of water-shared ion-pairs. The temperature dependent spectra in Figure 1B further reveal a blue-shift in the lowfrequency OH band, consistent with the weakening of the HOH···OH⁻ hydrogen bonds with increasing temperature.

The SC spectra of LiOH shown in Figure 2C,D are qualitatively similar to those of NaOH in Figure 2A,B, except for the lower intensity near 3500 cm<sup>-1</sup> for LiOH than for NaOH, which again reflects the greater ion-pairing in LiOH (and perhaps some influence of the Li<sup>+</sup> hydration-shell). Note that the concentration range of the aqueous LiOH solutions is smaller than that of the NaOH solution, due to the lower solubility of LiOH. Comparison of the concentration and temperature dependent SC spectra of aqueous LiOH indicates that the increased ion-pairing in LiOH at concentrations from 0.25 to 2 M is somewhat smaller than that induced by increasing the temperature from 5 to 100 °C at

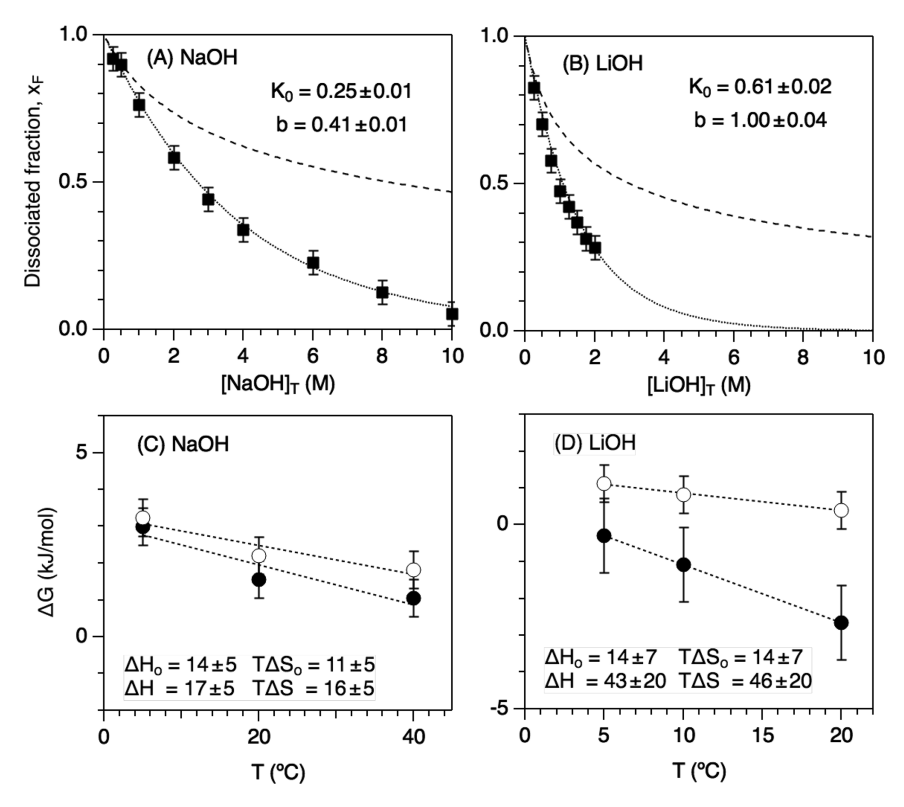


Figure 3. Ion-pair dissociation fractions  $x_F$  (A, B) and thermodynamics (C, D) obtained from concentration dependent changes in the Raman-MCR SC spectra intensity near 3500 cm<sup>-1</sup> in NaOH (A, C) and LiOH (B, D) solutions at 5 °C. The experimental square points in panels A and B are compared with theoretical predictions obtained assuming a concentration independent ion-pairing constant  $K_0$  (match to the experimental results at infinite dilution), as well as a best fit of the experimental results to eq 1, which assumes that the ion-pairing free energy decreases linearly with increasing concentration. The ion-pairing free energy  $\Delta G$ , enthalpy  $\Delta H$ , and entropy  $\Delta S$  (expressed in kJ mol<sup>-1</sup>) at 20 °C are obtained using eqs 3–6. The thermodynamic functions with a 0 subscript pertain to the dilute limit, and the nonsubscripted functions pertain to a 1 M solution.

0.5 M. The nearly zero intensity near 3500 cm<sup>-1</sup> in the SC spectra at 0.5 M and 100 °C again implies that this aqueous LiOH solution consists primarily of water-shared ion-pairs. Moreover, as in aqueous NaOH, the somewhat different concentration and temperature dependence of the low-frequency OH band indicates that some direct contact ion-pairs are formed at 2 M and 5 °C, while in a 0.5 M solution at 100 °C there are fewer direct contact ion-pairs and the HOH··· OH<sup>-</sup> hydrogen bonds are again weakened with increasing temperature.

The spectra shown in Figure 2 also reveal a peak near 3300 cm<sup>-1</sup> that becomes more evident at high concentrations and temperatures. This peak may perhaps be associated with the water OH groups in the first hydration-shell of OH<sup>-</sup> that are not hydrogen bonded to OH<sup>-</sup>. This assignment is supported by prior predictions of the Raman and IR spectra of aqueous NaOH and LiOH solutions, indicating that such first hydration-shell OH groups should have a vibrational frequency in this spectral range.<sup>1</sup>

Figure 3 shows results illustrating the more quantitative ion-pairing information that may be obtained from the concentration dependent Raman-MCR results shown in Figure 1A,C. The points in Figure 3 correspond to the experimentally determined fraction of dissociated ion-pairs,  $x_F = I/I_0$  (see eq 1). Again, this expression for  $x_F$  assumes that a fully formed water-shared ion-pair has a nearly vanishing intensity near 3500 cm<sup>-1</sup>, as implied by the highest-concentration and highest-temperature spectra shown in Figure 2. A comparison of the NaOH and LiOH results in Figure 3A,B clearly reveals

the greater degree of ion-pairing (lower  $x_F$  values) in aqueous LiOH than in aqueous NaOH.

The dashed curves in Figure 3A,B are predictions obtained assuming that the ion-pairing association constant is concentration independent,  $K_A = K_0$ , and has a value equal to that obtained from the experimental first derivative of  $\alpha_F$  with respect to [MOH]<sub>T</sub> at infinite dilution. The discrepancy between the dashed curves and the data points at higher concentrations indicates that the ion-pair association constants increase with increasing [MOH]<sub>T</sub>. The dotted curves in Figure 3A,B are obtained using eq 3, with  $\alpha_F$  and  $\alpha_F$  taken from quadratic fits to the  $\alpha_F$  values as a function of  $\alpha_F$  = [MOH]<sub>T</sub> (as further described in the SI).

Recall that b determines the linear increase in the ion-pairing free energy  $\Delta G$  with increasing ionic strength  $\mu \sim c_{\rm T}$ . A significantly poorer fit to the  $x_{\rm F}$  points is obtained if it is assumed that the ion-paring free energy scales with either  $\sqrt{\mu}$  or  $\sqrt{\mu}/(1-\sqrt{\mu})$ , rather than  $\mu$ . Moreover, when both a linear dependence and a square-root dependence are included in the fit, the linear coefficient invariably dominates.

The ion-pairing constants obtained using the results shown in Figure 3 may be compared with those previously obtained using potentiometric measurements. Specifically, ion-pairing association constants of NaOH and LiOH, extrapolated to infinite dilution, are  $K_0 = 0.25$  and 0.61 M<sup>-1</sup>, respectively. The factor of ~2.5 difference between these two  $K_0$  values is comparable to that obtained potentiometrically, although our  $K_0$  values are roughly a factor of 2 smaller than the potentiometric values.<sup>2</sup> Our results further indicate that the

ion-pairing equilibrium constant  $K_A$  invariably increases with concentration, as does the ratio of the LiOH and NaOH ion-pairing constants. For example, at  $[MOH]_T = 2$  M, the ion-pairing association constant ratio increases to  $K_A(\text{LiOH})/K_A(\text{NaOH}) \sim 8$ , as obtained using eq 3 with the coefficients shown in Figure 2 (and SI Table S1).

The lower two panels in Figure 3 show the experimental ion-pairing thermodynamic functions obtained using eqs 3–7, from the temperature and concentration dependence of  $x_F$ . Specifically, at each temperature the intensity near 3500 cm<sup>-1</sup> was fit to a quadratic function of concentration. The SC intensities were measured at five neighboring frequency values near 3500 cm<sup>-1</sup>, at each temperature and concentration. Results obtained at each of the five frequencies were used to obtain the average and standard deviation of  $K_0$  and b, as well as the corresponding ion-pairing thermodynamic function (as further described in the SI).

The plots in Figure 3C,D reveal that the ion-pairing free energy (obtained using eq 4) invariably decreases with increasing temperature, reflecting the increase in ion-pairing with increasing temperature. The negative slope of  $\Delta G$ indicates that  $\Delta S$  is positive (see eq 5). Since the magnitudes of  $T\Delta S$  are invariably larger than  $\Delta G$ , that further implies that  $\Delta H = \Delta G + T\Delta S$  is also invariably positive. Although there is significant uncertainty associated with the magnitudes of  $\Delta H$ and  $T\Delta S$ , their positive signs indicate that ion-pairing is enthalpically disfavored and entropically favored, contrary to ion-pairing in the gas phase that must be strongly enthalpically favored and entropically disfavored. Our results further imply that the magnitudes of the positive ion-pairing  $\Delta H$  and  $\Delta S$ values increase with increasing concentration, reflecting the larger solvent-mediated interactions in concentrated aqueous salt solutions.

#### SUMMARY AND DISCUSSION

Our Raman-MCR experiments and AIMD simulations have confirmed that ion-pairs in aqueous NaOH and LiOH solutions have a predominantly water-shared structure (rather than a direct contact or water-separated structure). The stability of these ion-pairs increases strongly with increasing temperature and is greater in LiOH than NaOH. The formation of the ion-pairs leads to a decrease in the hydration-shell spectral intensity near 3500 cm<sup>-1</sup>, in agreement with previously reported Raman-MCR and AIMD results. Our findings go beyond previous work in experimentally quantifying the ion-pairing equilibrium constant as a function of both concentration and temperature, to obtain the corresponding ion-pairing thermodynamic functions, as well as a more detailed description of the water-shared ion-pair structures.

Our observation that the ion-pairing free energy has an approximately linear concentration dependence appears to contradict the Debye–Hückel prediction that the activity coefficients of ions in water should scale as the square-root of ionic strength  $\sqrt{\mu}$ , or its generalizations by Davies and others. However, those predictions pertain to concentrations well below 1 M. The observed linear, rather than square root, dependence at higher concentrations is reminiscent of the fact that the experimental excess chemical potentials (solvation free energies) of various aqueous salt solutions are found to have an approximately quadratic dependence on  $\sqrt{\mu}$  (and thus an approximately linear

correlation with  $\mu$ ) at concentrations comparable to those of the present Raman-MCR measurements (see, for example, section 2.17 in ref 45).

We report the first measurements of  $\Delta H$  and  $T\Delta S$  for aqueous NaOH and LiOH, although prior potentiometric measurements have reported that ion-pairing in these solutions increases with increasing temperature, <sup>2,3</sup> thus confirming that  $\Delta S$  is positive. Moreover, some other aqueous ion-pairing processes have also been found to have positive  $\Delta H$  and  $\Delta S$  values. <sup>2,9</sup> Although our ion-pairing  $\Delta H$  and  $\Delta S$  are significantly uncertain, in part because of the assumption that the formation of a water-shared ion-pair fully depletes the SC spectral intensity near 3500 cm<sup>-1</sup>, relaxing that assumption is not expected to change the derived ion-pairing equilibrium constants by more than about a factor of 2 and, thus, would only change  $\Delta G$  by approximately  $-RT \ln 2$  (of the order of 1 kJ/mol). Thus, there is little doubt regarding our conclusion that both  $\Delta H$  and  $T\Delta S$  are positive and large compared to  $\Delta G$ .

Since the intrinsic interaction energy of the counterions with each other (in the absence of water) is necessarily negative, the observed positive sign of  $\Delta H$  must arise from water-mediated interactions. These may include both direct ion-water interactions and indirect ion-induced changes in water-water interactions. In the linear response (and dielectric continuum) approximation, direct ion-water interaction energies are predicted to be twice as large in magnitude as, and opposite in sign to, the corresponding indirect water-water interaction energies. 46 Thus, our experimentally observed positive sign of  $\Delta H$  implies that it arises from the decrease in the large negative direct ion-water interaction energy upon ion-pairing. Moreover, the fact that the magnitudes of  $\Delta H$  increase with increasing concentration indicates that direct ion-solvent interactions are larger in concentrated aqueous ionic solvents than in pure water. Similarly, the positive sign of  $\Delta S$  indicates that the thermally accessible configurational phase space available to the solution increases upon ion-pairing and is larger in concentrated aqueous NaOH and LiOH than at infinite dilution.

Our results suggest that Raman-MCR may be more generally applicable to other ion-pairing processes, as exemplified by the recent Raman-MCR investigation of the binding of Zn<sup>2+</sup>, Ca<sup>2+</sup>, and Mg<sup>2+</sup> to carboxylate anions.<sup>47</sup> Our thermodynamic results also imply that it can be a mistake to assume that ion-pairing in water is primarily driven by the electrostatic attraction between the oppositely charged ions. Rather, our results demonstrate that the ion-water interactions can dominate the resulting thermodynamics, leading to enthalpic destabilization of the ion-pair resulting from the loss of ion hydration energy, with a positive entropy change favoring ion-pairing. Thus, ion-pairing equilibrium constants and free energies can evidently be more significantly influenced by ion-water interactions than by the intrinsic electrostatic attraction of the oppositely charged counterions for each other. The latter conclusion is consistent with results obtained for some other aqueous ion-pairs<sup>2,9</sup> and may also contribute to the observed ion-pairing between two like-charge guanidinium cations,<sup>22</sup> as well as predictions of a water-shared free energy minimum in the ion-pairing potential of mean force between other like-charged ions in water<sup>23</sup> and at an air-water interface.<sup>24</sup>

#### ASSOCIATED CONTENT

## Supporting Information

The Supporting Information is available free of charge at https://pubs.acs.org/doi/10.1021/acs.jpcb.0c10564.

Thermodynamic analysis methods and results, additional experimental Raman-MCR spectra, and additional AIMD simulation predictions (PDF)

#### AUTHOR INFORMATION

#### **Corresponding Author**

Dor Ben-Amotz — Department of Chemistry, Purdue University, West Lafayette, Indiana 47907, United States; orcid.org/0000-0003-4683-5401; Email: bendor@purdue.edu

## **Authors**

Denilson Mendes de Oliveira — Department of Chemistry, Purdue University, West Lafayette, Indiana 47907, United States; © orcid.org/0000-0002-2579-8405

Aria J. Bredt – Department of Chemistry, Purdue University, West Lafayette, Indiana 47907, United States

Tierney C. Miller – Department of Chemistry and Biochemistry, University of Notre Dame, Notre Dame, Indiana 46556, United States

Steven A. Corcelli – Department of Chemistry and Biochemistry, University of Notre Dame, Notre Dame, Indiana 46556, United States; orcid.org/0000-0001-6451-4447

Complete contact information is available at: https://pubs.acs.org/10.1021/acs.jpcb.0c10564

#### Notes

The authors declare no competing financial interest.

#### ACKNOWLEDGMENTS

This work was supported by two National Science Foundation research grants, (CHE-1763581 for D.B.-A. and D.M.d.O.) and (CHE-1565471 for S.A.C.), as well as computing resources from the Extreme Science and Engineering Discovery Environment (TG-CHE190003) and high-performance computing resources and support from the Center for Research Computing at the University of Notre Dame. We also thank Aiming "Murphy" Zheng for assisting in the collection of preliminary results relevant to the present work, while she was an undergraduate research student. More generally, we would like to thank Lawrence Pratt for numerous stimulating discussions, including those that inspired one of us (DB-A) to get interested in ionic solvation thermodynamics over 20 years ago, and another one of us (SAC) when he was an undergraduate REU student with Lawrence Pratt in the summer of 1995.

# REFERENCES

- (1) Drexler, C. I.; Miller, T. C.; Rogers, B. A.; Li, Y. C.; Daly, C. A., Jr.; Yang, T.; Corcelli, S. A.; Cremer, P. S. Counter Cations Affect Transport in Aqueous Hydroxide Solutions with Ion Specificity. *J. Am. Chem. Soc.* **2019**, *141*, 6930–6936.
- (2) Gimblett, F. G. R.; Monk, C. B. E.M.F. Studies of Electrolytic Dissociation. Part 7 Some Alkali and Alkaline Earth Metal Hydroxides in Water. *Trans. Faraday Soc.* **1954**, *50*, 965–972.
- (3) Corti, H.; Crovetto, R.; Fernández-Prini, R. Aqueous Solutions of Lithium Hydroxide at Various Temperatures: Conductivity and Activity Coefficients. *J. Solution Chem.* **1979**, *8*, 897–908.

- (4) Corti, H. R.; Prini, R. F.; Svarc, F. Densities and Partial Molar Volumes of Aqueous Solutions of Lithium, Sodium, and Potassium Hydroxides up to 250°C. *J. Solution Chem.* **1990**, *19*, 793–809.
- (5) Nasirzadeh, K.; Neueder, R.; Kunz, W. Vapor Pressures and Osmotic Coefficients of Aqueous LiOH Solutions at Temperatures Ranging from 298.15 to 363.15 K. *Ind. Eng. Chem. Res.* **2005**, 44, 3807–3814.
- (6) Megyes, T.; Bálint, S.; Grósz, T.; Radnai, T.; Bakó, I.; Sipos, P. The Structure of Aqueous Sodium Hydroxide Solutions: A Combined Solution X-Ray Diffraction and Simulation Study. *J. Chem. Phys.* **2008**, *128*, 044501.
- (7) Hellström, M.; Behler, J. Concentration-Dependent Proton Transfer Mechanisms in Aqueous Naoh Solutions: From Acceptor-Driven to Donor-Driven and Back. *J. Phys. Chem. Lett.* **2016**, *7*, 3302—3306.
- (8) Shao, Y.; Hellström, M.; Yllö, A.; Mindemark, J.; Hermansson, K.; Behler, J.; Zhang, C. Temperature Effects on the Ionic Conductivity in Concentrated Alkaline Electrolyte Solutions. *Phys. Chem. Chem. Phys.* **2020**, 22, 10426.
- (9) Marcus, Y.; Hefter, G. Ion Pairing. Chem. Rev. 2006, 106, 4585-4621
- (10) Ben-Amotz, D. Hydration-Shell Vibrational Spectroscopy. J. Am. Chem. Soc. 2019, 141, 10569–10580.
- (11) Moskovits, M.; Michaelian, K. H. Alkali Hydroxide Ion Pairs. A Raman Study. J. Am. Chem. Soc. 1980, 102, 2209–2215.
- (12) van der Vegt, N. F. A.; Haldrup, K.; Roke, S.; Zheng, J. R.; Lund, M.; Bakker, H. J. Water-Mediated Ion Pairing: Occurrence and Relevance. *Chem. Rev.* **2016**, *116*, 7626–7641.
- (13) Tielrooij, K. J.; Garcia-Araez, N.; Bonn, M.; Bakker, H. J. Cooperativity in Ion Hydration. *Science* **2010**, 328, 1006–1009.
- (14) Okur, H. I.; Hladilkova, J.; Rembert, K. B.; Cho, Y.; Heyda, J.; Dzubiella, J.; Cremer, P. S.; Jungwirth, P. Beyond the Hofmeister Series: Ion-Specific Effects on Proteins and Their Biological Functions. *J. Phys. Chem. B* **2017**, *121*, 1997–2014.
- (15) Baer, M. D.; Fulton, J. L.; Balasubramanian, M.; Schenter, G. K.; Mundy, C. J. Persistent Ion Pairing in Aqueous Hydrochloric Acid. *J. Phys. Chem. B* **2014**, *118*, 7211–7220.
- (16) Roy, S.; Patra, A.; Saha, S.; Palit, D. K.; Mondal, J. A. Restructuring of Hydration Shell Water Due to Solvent-Shared Ion Pairing (Ssip): A Case Study of Aqueous MgCl<sub>2</sub> and LaCl<sub>3</sub> Solutions. *J. Phys. Chem. B* **2020**, 124, 8141–8148.
- (17) Agmon, N.; Bakker, H. J.; Campen, R. K.; Henchman, R. H.; Pohl, P.; Roke, S.; Thamer, M.; Hassanali, A. Protons and Hydroxide Ions in Aqueous Systems. *Chem. Rev.* **2016**, *116*, 7642–7672.
- (18) Hermansson, K.; Bopp, P. A.; Spångberg, D.; Pejov, L.; Bakó, I.; Mitev, P. D. The Vibrating Hydroxide Ion in Water. *Chem. Phys. Lett.* **2011**, *514*, 1–15.
- (19) Galib, M.; Baer, M. D.; Skinner, L. B.; Mundy, C. J.; Huthwelker, T.; Schenter, G. K.; Benmore, C. J.; Govind, N.; Fulton, J. L. Revisiting the Hydration Structure of Aqueous Na<sup>+</sup>. *J. Chem. Phys.* **2017**, *146*, 084504.
- (20) Kebede, G. G.; Mitev, P. D.; Broqvist, P.; Kullgren, J.; Hermansson, K. Hydrogen-Bond Relations for Surface OH Species. *J. Phys. Chem. C* **2018**, *122*, 4849–4858.
- (21) Mandal, A.; Tokmakoff, A. Vibrational Dynamics of Aqueous Hydroxide Solutions Probed Using Broadband 2DIR Spectroscopy. *J. Chem. Phys.* **2015**, *143*, 194501.
- (22) Vazdar, M.; Heyda, J.; Mason, P. E.; Tesei, G.; Allolio, C.; Lund, M.; Jungwirth, P. Arginine "Magic": Guanidinium Like-Charge Ion Pairing from Aqueous Salts to Cell Penetrating Peptides. *Acc. Chem. Res.* **2018**, *51*, 1455–1464.
- (23) Pratt, L. R.; Hummer, G.; Garciá, A. E. Ion Pair Potentials-of-Mean-Force in Water. *Biophys. Chem.* **1994**, *51*, 147–165.
- (24) Venkateshwaran, V.; Vembanur, S.; Garde, S. Water-Mediated Ion-Ion Interactions Are Enhanced at the Water Vapor-Liquid Interface. *Proc. Natl. Acad. Sci. U. S. A.* **2014**, *111*, 8729–8734.
- (25) Davis, J. G.; Gierszal, K. P.; Wang, P.; Ben-Amotz, D. Water Structural Transformation at Molecular Hydrophobic Interfaces. *Nature* **2012**, 491, 582–585.

- (26) Lawton, W. H.; Sylvestre, E. A. Self Modeling Curve Resolution. *Technometrics* 1971, 13, 617-633.
- (27) Perera, P.; Wyche, M.; Loethen, Y.; Ben-Amotz, D. Solute-Induced Perturbations of Solvent-Shell Molecules Observed Using Multivariate Raman Curve Resolution. *J. Am. Chem. Soc.* **2008**, *130*, 4576–4579.
- (28) Gierszal, K. P.; Davis, J. G.; Hands, M. D.; Wilcox, D. S.; Slipchenko, L. V.; Ben-Amotz, D. π-Hydrogen Bonding in Liquid Water. *J. Phys. Chem. Lett.* **2011**, *2*, 2930–2933.
- (29) Martínez, L.; Andrade, R.; Birgin, E. G.; Martínez, J. M. Packmol: A Package for Building Initial Configurations for Molecular Dynamics Simulations. *J. Comput. Chem.* **2009**, *30*, 2157–2164.
- (30) Hutter, J.; Iannuzzi, M.; Schiffmann, F.; VandeVondele, J. CP2K: Atomistic Simulations of Condensed Matter Systems. *Wiley Interdiscip. Rev. Comput. Mol. Sci.* **2014**, *4*, 15–25.
- (31) Daly, C. A.; Streacker, L. M.; Sun, Y.; Pattenaude, S. R.; Hassanali, A. A.; Petersen, P. B.; Corcelli, S. A.; Ben-Amotz, D. Decomposition of the Experimental Raman and Infrared Spectra of Acidic Water into Proton, Special Pair, and Counterion Contributions. J. Phys. Chem. Lett. 2017, 8, 5246–5252.
- (32) Hassanali, A.; Giberti, F.; Cuny, J.; Kühne, T. D.; Parrinello, M. Proton Transfer through the Water Gossamer. *Proc. Natl. Acad. Sci. U. S. A.* **2013**, *110*, 13723.
- (33) VandeVondele, J.; Krack, M.; Mohamed, F.; Parrinello, M.; Chassaing, T.; Hutter, J. Quickstep: Fast and Accurate Density Functional Calculations Using a Mixed Gaussian and Plane Waves Approach. *Comput. Phys. Commun.* **2005**, *167*, 103–128.
- (34) Goedecker, S.; Teter, M.; Hutter, J. Separable Dual-Space Gaussian Pseudopotentials. *Phys. Rev. B: Condens. Matter Mater. Phys.* **1996**, *54*, 1703–1710.
- (35) Hartwigsen, C.; Goedecker, S.; Hutter, J. Relativistic Separable Dual-Space Gaussian Pseudopotentials from H to Rn. *Phys. Rev. B: Condens. Matter Mater. Phys.* **1998**, *58*, 3641–3662.
- (36) Krack, M. Pseudopotentials for H to Kr Optimized for Gradient-Corrected Exchange-Correlation Functionals. *Theor. Chem. Acc.* 2005, 114, 145–152.
- (37) Becke, A. D. Density-Functional Exchange-Energy Approximation with Correct Asymptotic Behavior. *Phys. Rev. A: At., Mol., Opt. Phys.* **1988**, *38*, 3098–3100.
- (38) Lee, C.; Yang, W.; Parr, R. G. Development of the Colle-Salvetti Correlation-Energy Formula into a Functional of the Electron Density. *Phys. Rev. B: Condens. Matter Mater. Phys.* **1988**, 37, 785–789.
- (39) Grimme, S.; Antony, J.; Ehrlich, S.; Krieg, H. A Consistent and Accurate Ab Initio Parametrization of Density Functional Dispersion Correction (DFT-D) for the 94 Elements H-Pu. *J. Chem. Phys.* **2010**, *132*, 154104.
- (40) Daly, C. A.; Brinzer, T.; Allison, C.; Garrett-Roe, S.; Corcelli, S. A. Enthalpic Driving Force for the Selective Absorption of CO<sub>2</sub> by an Ionic Liquid. *J. Phys. Chem. Lett.* **2018**, *9*, 1393–1397.
- (41) Fega, K. R.; Wilcox, D. S.; Ben-Amotz, D. Application of Raman Multivariate Curve Resolution to Solvation-Shell Spectroscopy. *Appl. Spectrosc.* **2012**, *66*, 282–288.
- (42) Perera, P. N.; Browder, B.; Ben-Amotz, D. Perturbations of Water by Alkali Halide Ions Measured Using Multivariate Raman Curve Resolution. *J. Phys. Chem. B* **2009**, *113*, 1805–1809.
- (43) Davies, C. W. 397. The Extent of Dissociation of Salts in Water. Part VIII. An Equation for the Mean Ionic Activity Coefficient of an Electrolyte in Water, and a Revision of the Dissociation Constants of Some Sulphates. *J. Chem. Soc.* 1938, 2093–2098.
- (44) Sun, M. S.; Harriss, D. K.; Magnuson, V. R. Activity Corrections for Ionic Equilibria in Aqueous Solutions. *Can. J. Chem.* **1980**, *58*, 1253–1257.
- (45) Ben-Naim, A. Solvation Thermodynamics; Plenum Press: New York, 1987.
- (46) Ben-Amotz, D.; Underwood, R. Unraveling Water's Entropic Mysteries: A Unified View of Nonpolar, Polar, and Ionic Hydration. *Acc. Chem. Res.* **2008**, *41*, 957–967.

(47) Mendes de Oliveira, D.; Zukowski, S. R.; Palivec, V.; Hénin, J.; Martinez-Seara, H.; Ben-Amotz, D.; Jungwirth, P.; Duboué-Dijon, E. Binding of Biologically Relevant Divalent Cations to Acetate: Molecular Simulations Guided by Raman Spectroscopy. *Phys. Chem. Chem. Phys.* **2020**, 22, 24014–24027.